Dyes and Pigments 134 (2016) 41–50

Contents lists available at ScienceDirect

Dyes and Pigments

journal homepage: www.elsevier.com/locate/dyepig

New strategies for synthesis and immobilization of methalophtalocyanines onto kaolinite: Preparation, characterization and chemical stability evaluation

Tiago Honorato da Silva [a], Thalita F.M. de Souza [b], Anderson Orzari Ribeiro [b], Paulo Sergio Calefi [c], Katia Jorge Ciuffi [a], Eduardo José Nassar [a], Eduardo Ferreira Molina [a], Peter Hammer [d], Emerson Henrique de Faria [a, *]

[a] Gurpo de Pesquisa em Materiais Lamelares Híbridos -GPMatLam – Universidade de Franca, Av. Dr. Armando Salles Oliveira, Pq. Universitário, 201, CEP 14404-600, Franca, SP, Brazil
[b] Centro de Ciências Naturais e Humanas, Universidade Federal do ABC–UFABC, R. Santa Adélia 166, 09210-170, Santo André, SP, Brazil
[c] Instituto Federal de Educação, Ciência e Tecnologia de São Paulo – IFSP, Campus Sertãozinho, Rua Américo Ambrósio, Jd. Canaã, 269, CEP, 14169-263, Sertãozinho, SP, Brazil
[d] Instituto de Química, UNESP-Universidade Estadual Paulista, 14800-900, Araraquara, SP, Brazil

ARTICLE INFO

Article history:
Received 9 March 2016
Received in revised form
18 June 2016
Accepted 27 June 2016
Available online 28 June 2016

Keywords:
Phtalocyanines
Immobilization
Hybrid materials
Clays
Nanocomposites

ABSTRACT

This study presents results concerning the one-step synthesis and immobilization of a metallophthalocyanine on kaolinite as support/catalyst. X-ray diffractometry (XRD), nuclear magnetic resonance (NMR) and infrared (FTIR), UV/Visible (UV/Vis) and X-ray photoelectron (XPS) spectroscopies, thermal analyses, textural analyses (BET) and scanning electron microscopy (SEM) aided for the characterization of the materials. The FTIR, XPS and UV/Vis absorption spectra confirmed metallophthalocyanine formation. XRD analysis provided data on the structural disorganization of kaolinite during the synthesis of metallophthalocyanine, corroborated by SEM. NMR revealed that partial dissolution of aluminum from the octahedral kaolinite sheets was possible, which should release Al into the medium and, together with phthalonitrile, promote cyclomerization of the phthalocyanine macrocycle.

1. Introduction

Phthalocyanines are symmetric aromatic macrocycles consisting of benzopyrrole rings connected by nitrogen bonds [1,2]. This arrangement gives rise to a π electron conjugation that provides phthalocyanines with high absorption coefficient in the UV/Visible region, stable electron configuration, and excellent optical properties [3,4].

The first methods developed for the synthesis of metallophthalocyanines involved slow reactions that required high temperatures. In most cases, these conditions culminated in relatively low yields because the reactants underwent degradation and subproducts emerged in the reaction medium [5]. Over the last decades, new techniques have been developed to increase process yield and make the synthesis of metallophthalocyanines more selective. For example, cyclotetramerization of precursors derived from phthalonitriles, phthalimides, phthalic anhydride, and others has enabled the synthesis of metallophthalocyanines in moderate yields [6,7].

In aqueous medium, metallophthalocyanines form aggregates that make dispersion difficult. Methalophthalocyanine immobilization on inorganic matrixes minimizes this issue, reaching the atomic molecular scale. Moreover, immobilization increases thermal and chemical stability, improving the properties of metallophthalocyanines [8,9].

The synthetic routes available to prepare metallophthalocyanines demand significantly long purification steps and excessive amounts of energy. These routes also require the use of a variety of solvents and metallic salts or metals for phthalocyanine cyclomerization, which can contaminate the environment. To meet the principles of green chemistry and sustainability when synthesizing metallophthalocyanines, researchers have searched for new

* Corresponding author.
E-mail address: eh.defaria@gmail.com (E.H. de Faria).

http://dx.doi.org/10.1016/j.dyepig.2016.06.044
0143-7208/

routes that demand less energy and little or no metal or metallic salt as the starting reactant. Another research activities aimed to improve the properties of metallophthalocyanines by immobilizing them on inorganic matrixes [10].

The use of inorganic matrixes as a source of metallic ions for metallophthalocyanine cyclomerization has become an interesting alternative—matrixes can donate metal ions and act as support/catalyst for the synthesized metallophthalocyanines, promoting immobilization and enhancing the physicochemical properties of these macromolecules.

Clay minerals have been commonly employed as support to immobilize many substances [11–13]. In this context, kaolinite has stood out for its natural abundance, physicochemical properties, and lamellar structure. Kaolinite constitutes an important industrial raw material for immobilization of metallophthalocyanines [10], porphyrins [14,15], and other complexes [16], to generate hybrid organic-inorganic materials with interesting properties.

Motivated by the possibility of obtaining metallophthalocyanines by new synthetic routes, in this work we present the preparation and immobilization of metallophthalocyanine on kaolinite in a single step, aiming to save energy, reduce solvent consumption, and comply with the principles of green chemistry and sustainability.

Driven by the ability to synthesize metallophthalocyanines by new synthetic routes, this work shows the study of the aluminum metallophthalocyanines synthesis using kaolinite as aluminium source and support, the immobilization of the synthesized complex in a single step are discussed, aiming energy saving, solvent and while reaching the precepts of green and sustainable chemistry, wherein the aluminium was generated in situ during the synthesis.

The solids could be applied as heterogeneous catalysts, and in photodinamic therapy, photooxidation reactions and photodegradation of pollutants. The great problem in use conventional metallophtalocyanines is the aglomeration of these complexes. However using the complexes imobilized into layered kaolinite we prevent the agregation in the axial position and also increase the activity.

2. Experimental

The procedures used to purify the clay mineral and to intercalate dimethylsulfoxide (DMSO) into its interlayer space were carried out as described in other literature articles authored by members of our research team [10,17].

2.1. Synthesis and immobilization of metallophthalocyanine on kaolinite

Phthalonitriles, which are precursors of phthalocyanines, bear groups that can interact with groups in the kaolinite structure. This allows immobilization of the precursor on the matrix, followed by metallophthalocyanine formation. One-step synthesis and immobilization of metallophthalocyanines on kaolinite required the use of kaolinite intercalated with DMSO (KaDMSO) and 4-nitrophthalonitrile ($PCNO_2$) at a 3:1 KaDMSO/$PCNO_2$ (m/m) ratio. This mixture was kept at 150 °C for 48 h. After washing with acetone and separation by centrifugation, the resulting material (designated $KaPCNO_2$) was characterized. Data were compared with the results obtained for aluminum (III) tetranitrometallophthalocyanine (Al(III)TNMPc) obtained by conventional route using solvent and conventional aluminium source from metallic salt according Shaposhnikov [18], that consisting in react one organic ligand that containing nitro groups (4-nitrophthalonitrile) in contact with metallic specie at temperature near to 210–220 °C. Fig. 1 shows a schematic representation of the new synthetic route used to prepare and immobilize metallophthalocyanine on kaolinite.

2.2. Characterization techniques

The powder X-ray diffractograms (PXRD) of the solids were recorded on a Miniflex II–RIGAKU diffractometer operating at 30 kV and 15 mA (1200 W), using filtered Cu Kα radiation (λ = 1.54 Å). The angle 2θ varied from 2 to 65°. All the analyses were undertaken at a scan rate of 2° (2θ) per minute.

Thermal analyses were performed on a TA Instruments–SDT Q600–Simultaneous DTA-TGA analyzer. The samples were heated from 25 to 900 °C at a heating rate of 20 °C per minute, in oxidizing (air) atmosphere, at a flow rate of 100 mL/min.

Infrared (FTIR) absorption spectra were acquired on a Perkin Elmer FT-IR Frontier Spectrometer by using a diffuse reflectance accessory. Detailing, 1 mg of each solid were mixed with 100 mg of KBr and finely pulverized until the complete dilution of each solid in KBr. Solids rich in organic ligands (e.g. aluminium metallophthalocyanine were diluted 0.1 mg with 100 mg of KBr. The powder obtained in a typical holder and finally the samples inserted in the FTIR equipment and analyzed The number of scans acquisitions were 32 per spectrum the resolution of 1 cm^{-1} was employed.

For the ultraviolet/visible (UV/Vis) absorption spectra, the

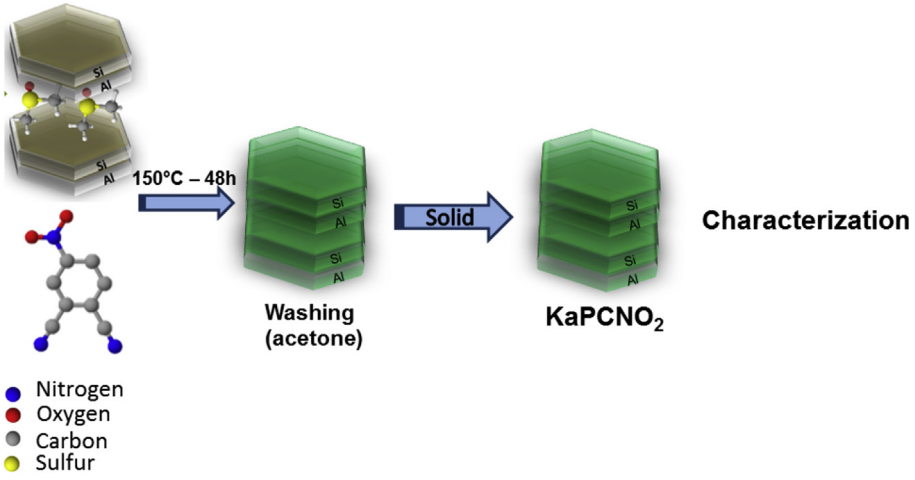

Fig. 1. Schematic representation of the new synthetic route used to prepare and immobilize metallophthalocyanine on kaolinite.

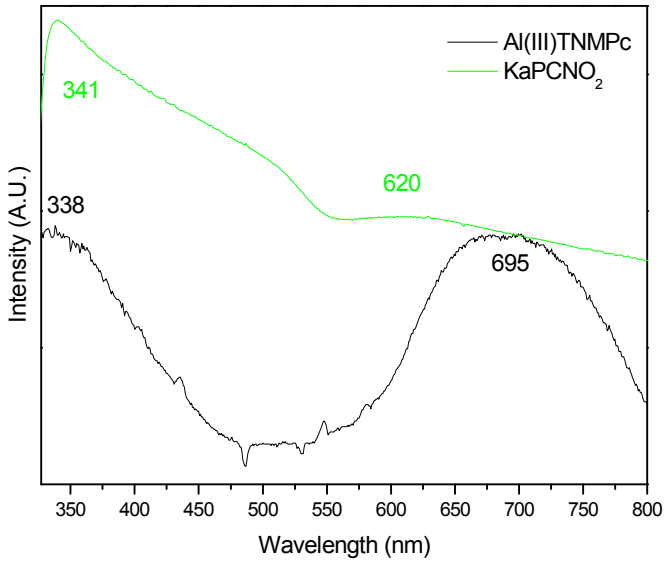

Fig. 2. UV/Vis spectra of Al(III)TNMPc and $KaPCNO_2$.

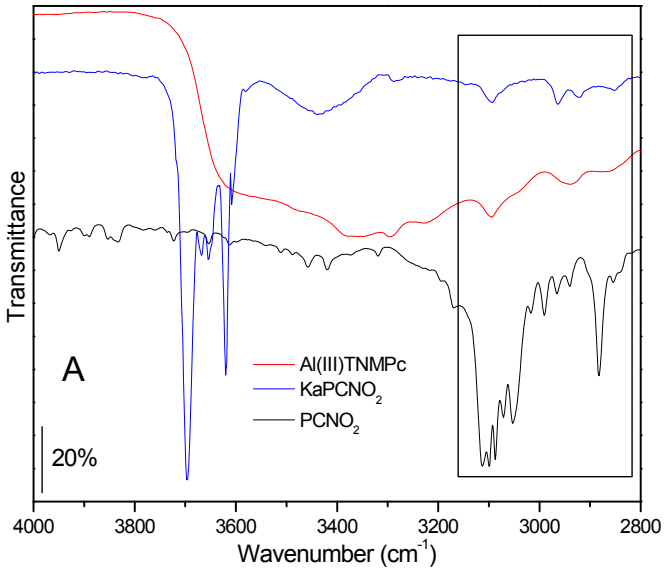

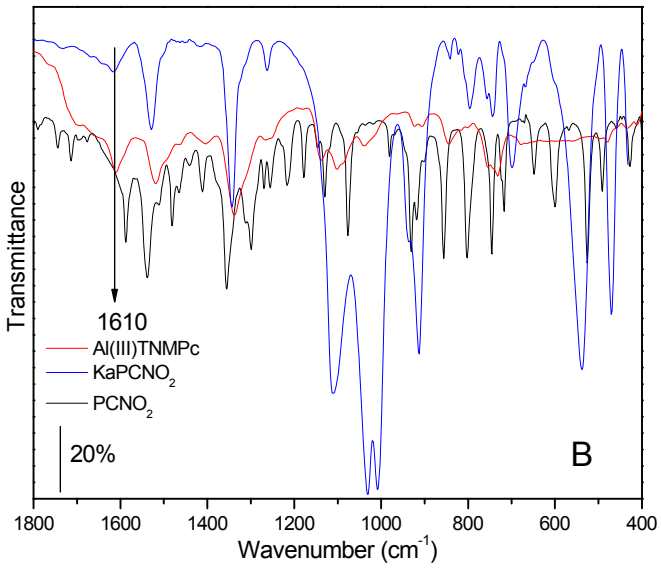

Fig. 3. FTIR absorption spectra of Al(III)TNMPc, Ka, $KaPCNO_2$, and $PCNO_2$ separated by regions: A – from 4000 cm^{-1} to 2800 cm^{-1}; B – from 1800 cm^{-1} to 400 cm^{-1}.

samples were placed in cells with 10-mm optical path length. The spectra of liquid and solid samples were recorded on a DiodeArray UV–Vis spectrophotometer HP mod. 8453 and on an OceanOptics Fluorimeter, respectively.

The X-ray photoelectron spectroscopy (XPS) was carried out at a pressure of less than 10^{-7} Pa using a commercial spectrometer (UNI-SPECS UHV). The Mg Kα line was used ($h\nu = 1253.6$ eV) and the analyzer pass energy was set to 10 eV. The inelastic background of the Al 2p, Si 2p, N 1s, O 1s and C 1s electron core-level spectra was subtracted using Shirley's method. The binding energy scale of the spectra was corrected using the C 1s hydrocarbon component of the fixed value of 285.0 eV. The spectra were fitted without placing constraints using multiple Voigt profiles.

Nuclear magnetic resonance spectra were registered on a Bruker apparatus model AVANCE III, 9.4 Tesla (400 MHz for hydrogen frequency), equipped with a 4-mm CP/MAS probe for solid samples and a 10-mm BBO probe for liquid samples.

Scanning electron microscopy images were obtained on a TESCAN VEJA 3 SBH apparatus equipped with 30-kV W filament, (3-nm resolution), and SE and BSE detectors.

The textural analyses were accomplished from the corresponding nitrogen adsorption/desorption isotherms at −196 °C, obtained in a static volumetric apparatus (Micromeritics Model ASAP 2020 adsorption analyzer). The samples (0.2 g) were degassed at 150 °C for 24 h. The specific surface area (S_{BET}) was obtained by the BET method, and the total pore volume was calculated from the amount of nitrogen adsorbed at a relative pressure of 0.95.

3. Results and discussion

Characterization of Ka and KaDMSO provided results that agreed with literature data and confirmed the lamellar nature of kaolinite and DMSO intercalation into the clay [10,17].

3.1. UV/Vis absorption spectroscopy

Fig. 2 shows the UV/Vis spectra of $KaPCNO_2$ and Al(III)TNMPc. These spectra confirmed formation of the metallophthalocyanine.

Both spectra displayed the typical bands of metallophthalocyanines: the Soret band between 300 and 350 nm and the Q band between 600 and 700 nm [3,4]. More specifically, these bands were located at 338 and 695 nm in the spectrum of Al(III)TNMPc, respectively, and at 341 and 620 nm in the spectrum of $KaPCNO_2$, respectively. Comparison of the two spectra and the band shifts evidenced formation of the metallophthalocyanine and its immobilization on the functionalized kaolinite.

3.2. FTIR spectroscopy

Fig. 3 and Table 1 display the FTIR spectra and the major band assignments for Al(III)TNMPc, Ka, $KaPCNO_2$, and $PCNO_2$, respectively.

The FTIR spectra also attested to metallophthalocyanine formation. Bands due to C=N group vibration emerged at 1616 and 1611 cm^{-1} for $KaPCNO_2$ and Al(III)TNMPc, respectively, while the spectrum of the precursor $PCNO_2$ did not contain this band. The vibrations related to the NO_2 group appeared at 1337, 1405, 1520, and 3094 cm^{-1} in the spectrum of Al(III)TNMPc, and at 1344, 1421, 1527, and 3097 cm^{-1} in the spectrum of $KaPCNO_2$. As for $PCNO_2$, the

Table 1
Assignment of the main FTIR absorption bands.

	Ka (cm^{-1})	Al(III)TNMPc (cm^{-1})	$PCNO_2$ (cm^{-1})	$KaPCNO_2$(cm^{-1})
υOH $_{inter}$	3696	–	–	3697
υOH $_{intra}$	3668, 3654, 3620	–	–	3668, 3654, 3620
υN=O	–	1337, 1405, 1520, 3094	1356, 1411, 1538, 3085-3116	1344, 1421, 1527, 3097
υC=N	–	1611		1616

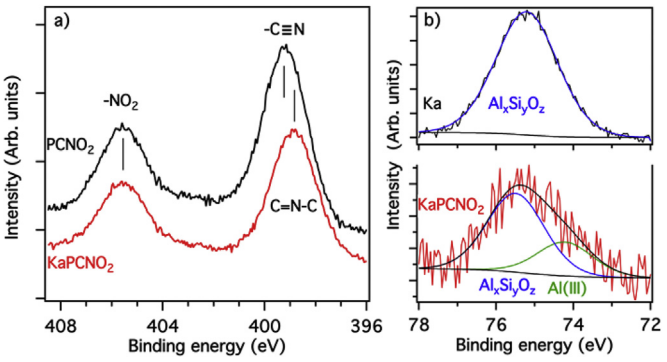

Fig. 4. XPS a) N 1s spectra of $PCNO_2$ and $KaPCNO_2$, b) fitted Al 2p spectra of Ka and $KaPCNO_2$.

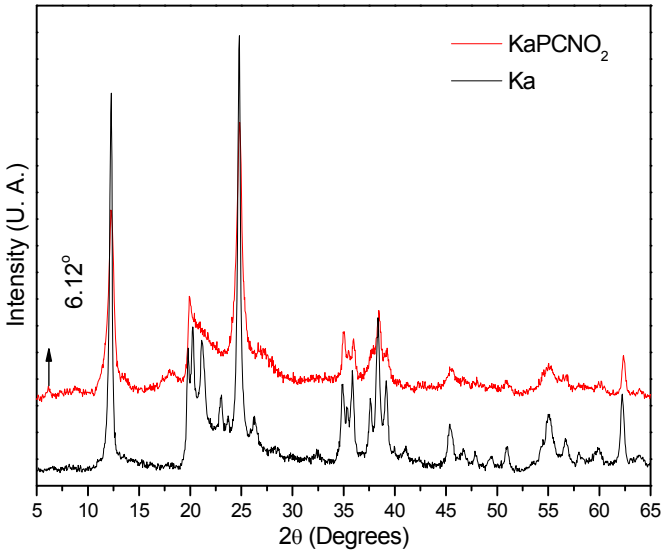

Fig. 5. Diffractograms of Ka and $KaPCNO_2$.

bands due to N=O group vibration arose at 1356, 1411, and 1538 and between 3085 and 3116 cm^{-1} [18–21]. The changes observed and displacements in the FTIR spectra of the solids compared to kaolinite confirm the interaction of NO_2 groups from Al(III)TNMPc synthesized in situ with kaolinite interlayer hydroxyl groups.

3.3. XPS analysis

Additional evidence for the formation of aluminum(III) phthalocyanine was obtained by the analysis of XPS N 1s and Al 2p core-level spectra. Fig. 4a displays the N 1s spectra obtained for the $PCNO_2$ precursor and the $KaPCNO_2$ product. For $PCNO_2$ the component related to nitric oxide, located at 405.5 eV, is separated form the nitrile group (399.2 eV) by about 6.3 eV [22]. The formation of pyrrole-like bonds (C=N–C) induces a shift of the low binding energy component to 398.7 eV [22] Another indication for the extraction of Al(III) from kaolinite under formation of

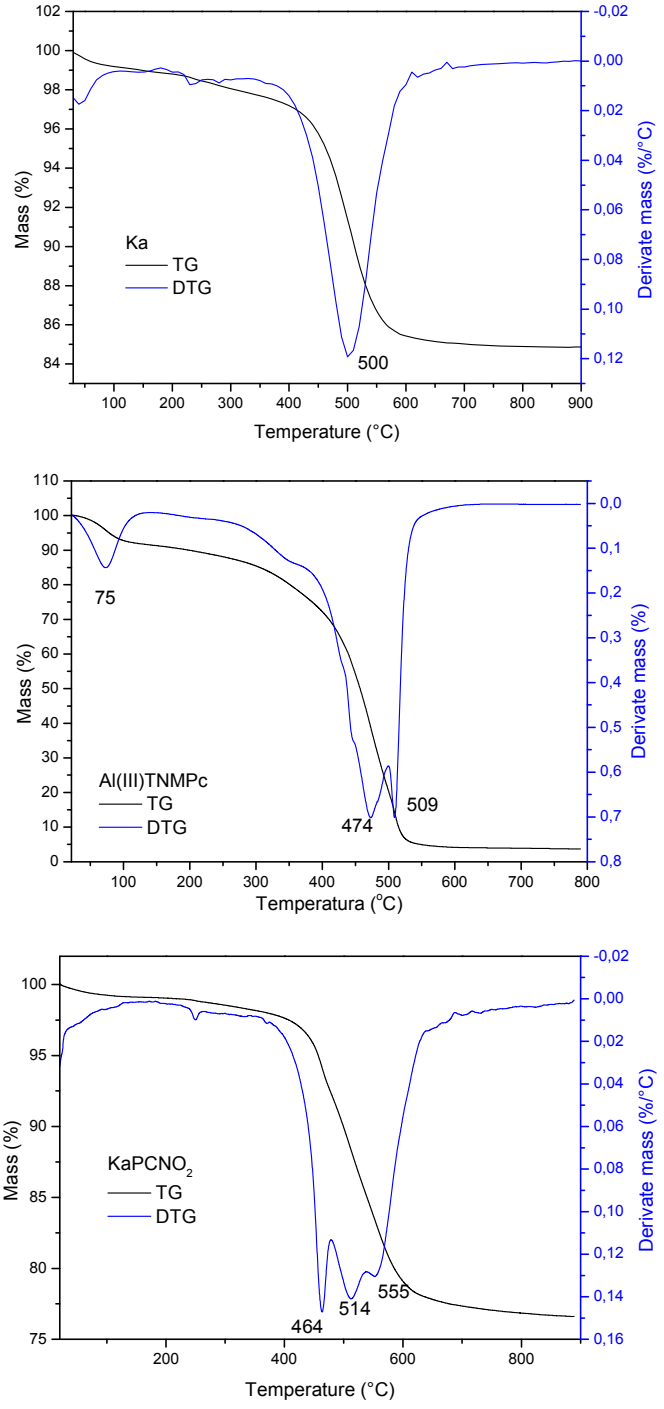

Fig. 6. TG/DTG curves obtained for Ka, Al(III)TNMPc, and $KaPCNO_2$.

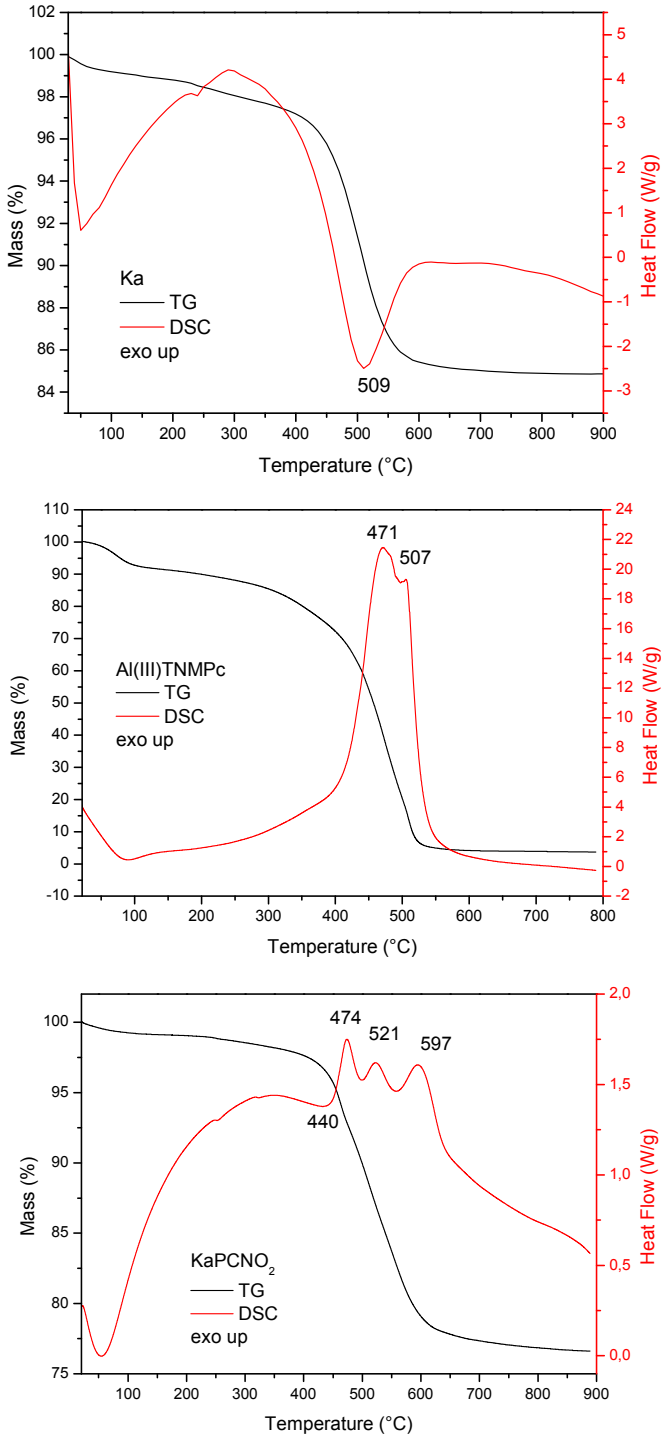

Fig. 7. TG/DTA curves obtained for Ka, Al(III)TNMPc, and $KaPCNO_2$.

aluminum(III) phthalocyanine comes from the Al 2p spectra, when comparing kaolinite with $KaPCNO_2$. The spectrum of Ka can be fitted with a single component at 75.3 eV, related to Al of the octahedral sheets bonded to Si occupying the tetrahedral layer [22]. The low energy component (74.2 eV), detected in the spectrum of $KaPCNO_2$, is indicative for Al(III) species in metallophtalocyanine. Taking in account the low sampling depth of XPS of about 5 nm, the noisy Al 2p spectrum of $KaPCNO_2$ results from attenuation effect of kaolinite caused by the wrapping effect of phtalocyanine macromolecules. Furthermore, the quantitative analysis confirmed the nominal composition of TNMPc (61.5 at.% C, 23.1 at.% N, 15.4 at.% O), within an error of ±10%. No signal of sulfur was detected in the spectra, indicating the absence of residual DMSO.

3.4. XRPD analysis

Fig. 5 depicts the diffractograms recorded for Ka and $KaPCNO_2$. The XRD patterns evidenced the structural modifications that the metallophthalocyanine synthesis promoted in kaolinite.

The diffractograms of KaDMSO and $KaPCNO_2$ were different. Structural modifications experienced by kaolinite during metallophthalocyanine synthesis were evident in the diffractogram of $KaPCNO_2$. Crystalline order decreased during the synthesis—the peaks due to reflections d_{020} and d_{002} broadened, and the peak relative to reflection d_{111} disappeared. Therefore, metallophthalocyanine synthesis made kaolinite more disorganized due to clay exfoliation/delamination and/or partial dissolution [10,23–25]. The low-intensity peak at $2\theta = 6.12°$, corresponding to a basal spacing of 14.42 Å, was compatible with metallophthalocyanine intercalated into kaolinite interlayer space, obviously this space is not compatible with perpendicular orientation of Al(III)TNMPc, probably this large complex presents parallel orientation in relation to interlayer space of clay. The same effect was previously observed in the previous work using metalloporphryins into grafted clay [15]. Another point that could be emphasized is that treatment removes completely the DMSO molecules from interlayer space of kaolinite and results in the small effect at 14.42 Å assigned to 4-nitrophthalonitrile intercalated and also the parallel orientated Al(III)TNMPc into kaolinite interlayer spaces.

3.5. Thermal analyses

Fig. 6 presents the TG/DTG curves obtained for Ka, $KaPCNO_2$ and Al(III)TNMPc. Comparison of the thermal analyses of Ka and $KaPCNO_2$ revealed that have similar profiles, with small differences due to the presence of the metallophthalocyanine (Al(III)TNMPc).

The TG/DTG curves of Al(III)TNMPc showed a mass loss below 100 °C, due to moisture water, as well as mass losses relative to metallophthalocyanine degradation at maximum temperatures of

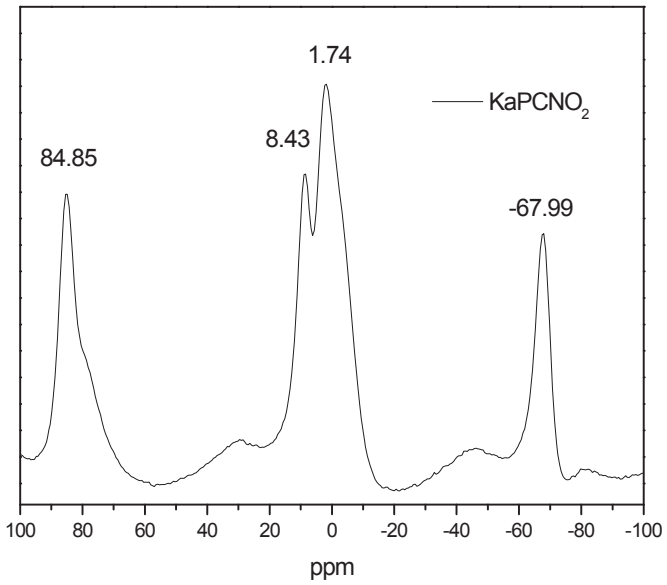

Fig. 8. ^{27}Al NMR spectrum of $KaPCNO_2$.

474 and 509 °C. Comparison of the TG/DTG profiles of $KaPCNO_2$ and Al(III)TNMPc showed that the thermal events occurred at similar temperatures. Because the metallophthalocyanine degradation temperatures were close to the temperature at which kaolinite dehydroxylation took place, the mass losses at 464, 514, and 555 °C could result from both metallophthalocyanine degradation and the dehydroxylation process. However, analysis of the TG/DTG curves of $KaPCNO_2$ showed that this material contained organic matter—the percent mass loss of purified Ka and $KaPCNO_2$ was 15 and 24%, respectively, and the higher mass loss in the case of $KaPCNO_2$ could be due to the presence of the metallophthalocyanine synthesized in situ on kaolinite.

Based on this mass loss and as demonstrated in the literature [26], it was possible to calculate the amount of synthesized metallophthalocyanine – 1.05 mol of metallophthalocyanine per mol of kaolinite.

The DTA curves (Fig. 7) obtained for Ka showed an endothermic mass loss at 509 °C, due to kaolinite dehydroxylation. For Al(III) TNMPc, there were two exothermic processes, at 471 and 507 °C, ascribed to aluminum(III) tetranitrometallophthalocyanine. As for $KaPCNO_2$, the kaolinite dehydroxylation temperature decreased (440 °C) as a result of $PCNO_2$ reacting with kaolinite. The temperatures at which exothermic Al(III)TNMPc degradation occurred increased because kaolinite conferred protection to the aluminum complex immobilized on the clay, consequently improving the thermal stability of the metallophthalocyanine.

3.6. ^{27}Al NMR analysis

NMR is an important tool to characterize hybrid materials based on kaolinite. This technique evidences changes in the intensities and chemical shifts of octahedral (hexacoordinated) aluminum species, which are coordinated with reaction-prone hydroxyls present in the octahedral sheet [27]. Fig. 8 shows the ^{27}Al NMR spectrum of $KaPCNO_2$.

The peaks with chemical shifts of 1.74 and 8.43 ppm were

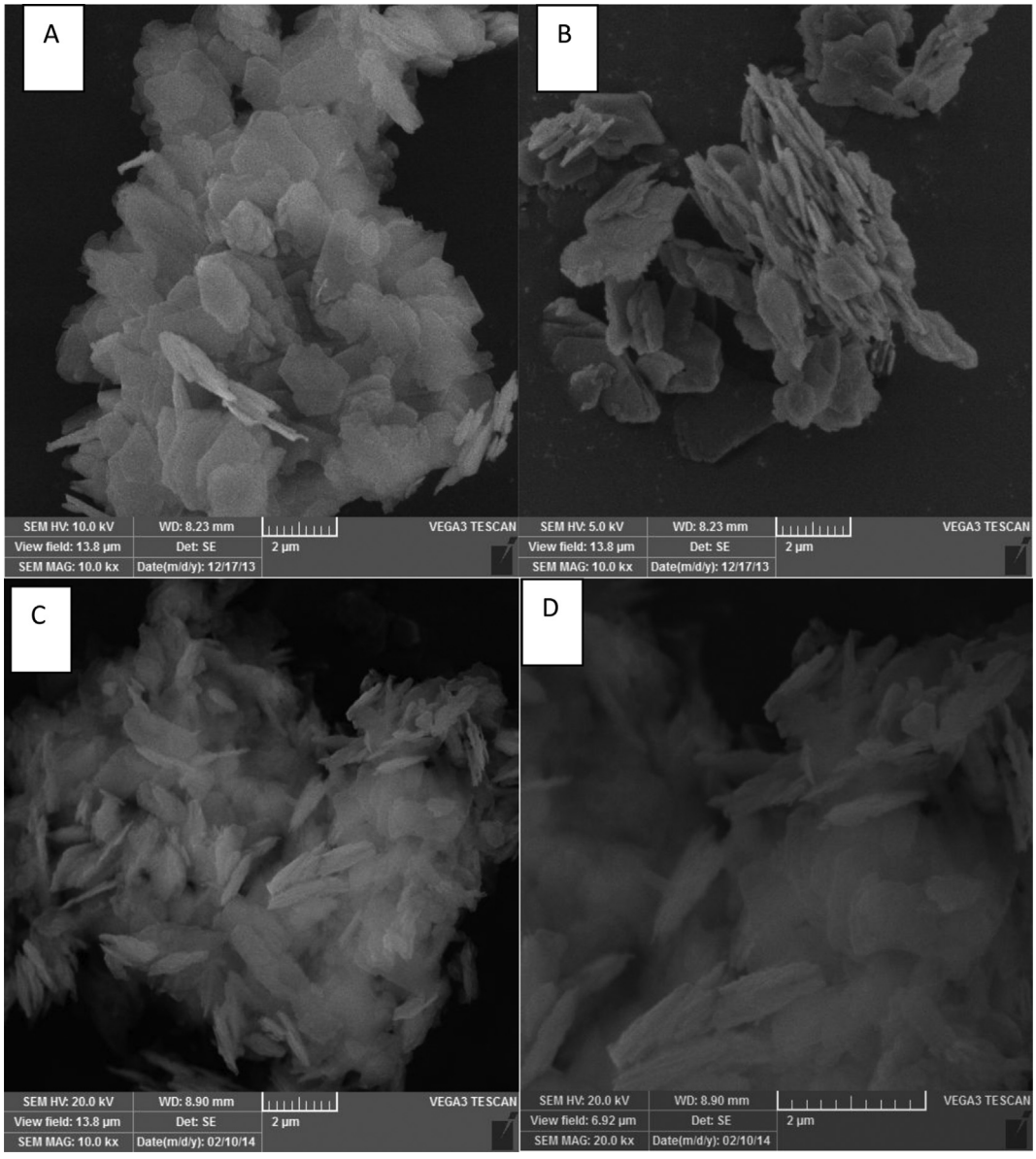

Fig. 9. SEM images of Ka (A and B) and $KaPCNO_2$ at 10kx (C) and 20kx (D) magnification.

assigned to hexacoordinated (octahedral) aluminum in the kaolinite octahedral sheet [28,29]. Fitzgerald et al. [29] demonstrated that the relation between octahedral and tetrahedral aluminum (relative intensities in the spectrum) was 400:1 for kaolinite. This was not the case for $KaPCNO_2$—the peaks due to tetrahedral aluminum were practically as intense as the peaks due to octahedral aluminum. Using an average value to calculate the ratio between octahedral and tetrahedral aluminum, the obtained ratio was approximately 1.4:1. These differences between kaolinite and the material synthesized herein may have stemmed from partial dissolution of aluminum present in the octahedral sheet during metallophthalocyanine synthesis, as judged from the chemical shifts at −67.99 and 84.85 ppm, due to tetracoordinated aluminum [29,30]. Hence, free aluminum dissolved in the octahedral sheet might exist and participate in the phthalocyanine macrocycle cyclomerization, affording a metallophthalocyanine that bears aluminum as the central ion.

Lyubimtsev et al. [31]. examined the reactivity of phthalonitriles derivatives containing different terminal groups to promote the phthalocyanine synthesis by conventional routes; for example,

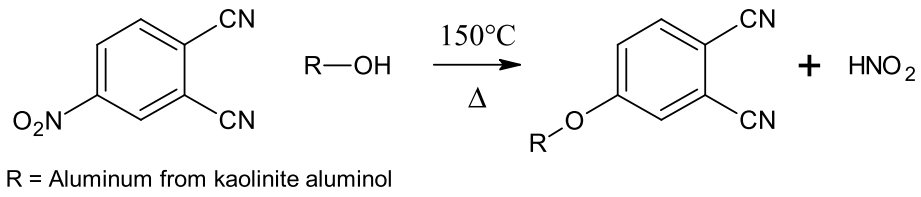

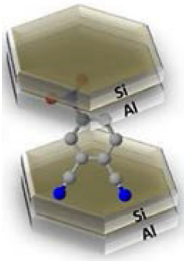

Fig. 10. Schematic representation of the first stage of in situ kaolinite-immobilized metallophthalocyanine synthesis.

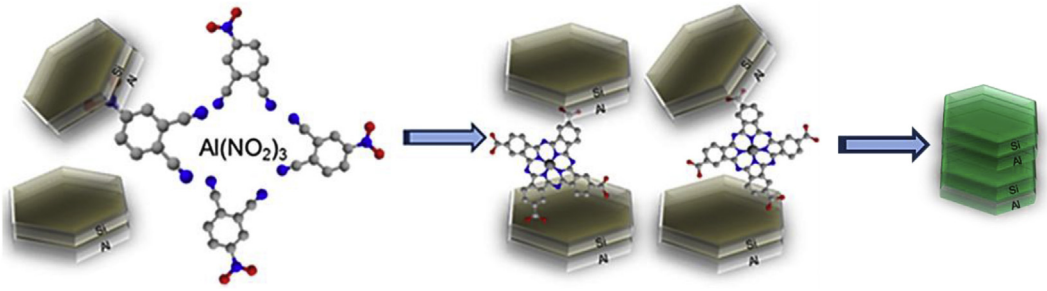

Fig. 11. Schematic representation of the third stage of in situ kaolinite-immobilized metallophthalocyanine synthesis.

Fig. 12. Kaolinite functionalized with aluminum(III) tetranitrometallophtalocyanine.

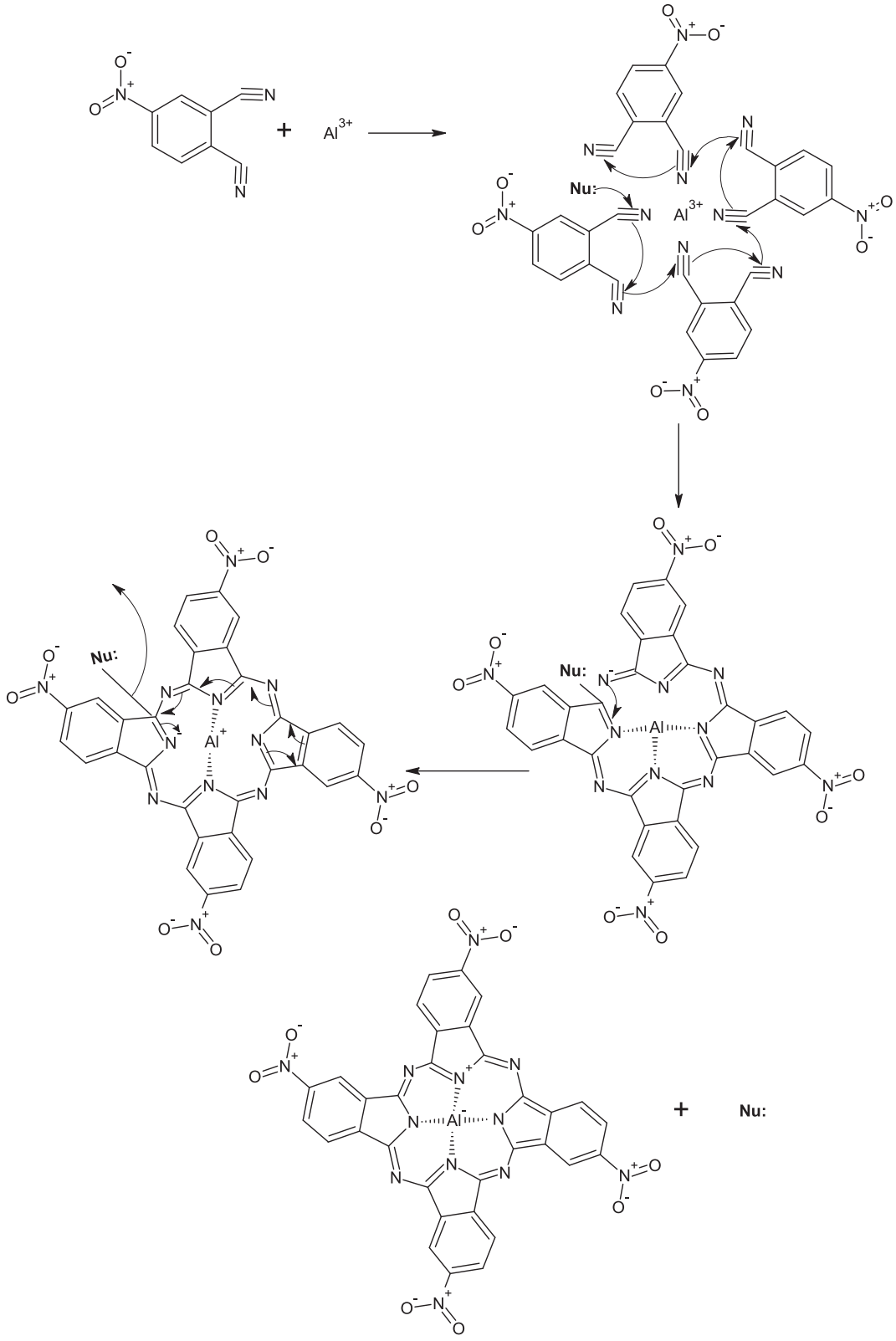

Fig. 13. Cyclization reaction mechanism for aluminum(III) metallophthalocyanine formation.

the 4-nitrophthalonitrile and 4-aminophtalonitrile, yielding results that demonstrate that the nitro group could influence the reactivity of the composite, the reaction rate is very bigger when use the derivative containing nitro group. Based on this theoretical and experimental result and based on the present s study, we propose that by promoting the reaction of the 4-nitrophthalonitrile with kaolinite, it has the ability to dissolve partially the octahedral sheet of this clay mineral, inducing the leaching of Al^{3+}, consequently

promoting the cyclomerization reaction without use conventional presence of metallic salts and solvents.

3.7. SEM analysis

SEM provided information about the morphology of the prepared materials. Fig. 9 presents the SEM images obtained for $KaPCNO_2$ and Ka.

$KaPCNO_2$ was fragmented into poorly aggregated hexagonal sheets, forming a layered material with few pillared layers. Particles were smaller and less ordered as compared with Ka (Fig. 9A and B). These results agreed with XRD data and indicated that kaolinite was exfoliated/delaminated or even partially dissolved during metallophthalocyanine synthesis.

3.8. Mechanism investigation

The analysis conducted in this study led us to propose a mechanism involving simultaneous metallophthalocyanine synthesis and immobilization on kaolinite. The stages of the proposed process are as follows (Figs. 10 and 11):

1st stage: The nitro group of 4-nitrophthalonitrile reacts with kaolinite, to functionalize part of the kaolinite lamellae with phthalonitrile and to generate nitrous acid as the reaction subproduct.

2nd stage: Nitrous acid reacts with nonfunctionalized aluminol, to dissolve part of the kaolinite octahedral sheets and to generate aluminum nitrite according to the following reaction:

$$Al{-}OH + HNO_2 \rightarrow Al(NO_2)_3 + H_2O$$

3rd stage: For metallophthalocyanine synthesis to occur, it is necessary to add a metallic salt or a metal to the reaction medium. In the present case, addition of a metallic salt was dismissed because a salt originated in the reaction medium during the metallophthalocyanine synthesis. Indeed, the reaction medium contained kaolinite functionalized with 4-nitrophthalonitrile, nonfunctionalized kaolinite, 4-nitrophthalonitrile (added in excess), and aluminum nitrite (which emerged during the synthesis) (Fig. 11). This mixture was kept at 150 °C for 48 h, to afford a green solid whose color was typical of metallophthalocyanine (see Fig. 12)

The nitronium group is an intermediate state. The nitronium were generated from nitrosil groups from 4-nitrphthallonitrile precursor, when this specie attack the $Al(OH)_3$ from gibbsite kaolinite layer. The possible mechanism, certainly involves the dissolution of aluminium from kaolinite promoted by nucleophillic attack of nitrosil group to kaolinite layers generating in situ the acidic specie that could remove the aluminium from gibbsite layer (this acidic specie are generated in situ), as represented in the scheme in Fig. 12. The nitronium group generated before interaction with kaolinite gibbsite layer (will act as nucleophile) used at the start of the cyclization oxidizes nitrite to nitrate by donating two electrons to the macrocyclic complex. The resulting nitronium ions undergo aromatic electrophilic substitution at position 4 or combine with another nitronium ion, to produce a nitrogen molecule ($N_{2(g)}$). N_2 then participates in a substitution reaction, to form a nitrate monophthalocyanine and hydrogen gas.(See Fig. 13)

The nitronium are not stable and could origin the nitrite and nitrate ions. This oxidation process could be probably induced by kaolinite which one oxidant environment, and also induced by molecular oxygen from atmosphere. Is important remark that nitronium is one intermediate state and at final we have present only the nitrite or nitrate ions.

Table 2
Specific surface area (S_{BET}) and pore size (V_{pTotal}) using the BET method of kaolinite, kaolinite intercalated with DMSO and compound grafted with $PCNO_2$.

Sample	$S_{BET}(m^2/g)$	Pore size (Å)
Ka	15.6	179
Ka-DMSO	4.2	806
Ka-$PCNO_2$	0.3	729

^{27}Al NMR and TG data attested to the synthesis of metallophthalocyanine catalyzed by kaolinite and reinforced our proposal that Al(III)TNMPc synthesis and immobilization occurred simultaneously. Indeed, the metallocomplex decomposed at higher temperature than the phthalonitrile precursor. The amount of metallophthalocyanine was calculated from the residue obtained from the thermogravimetric curve [26]. The minimum formula based on the molar ratio Ka/Al(III)TNMPc was Ka-$(Al(III)TNMPc)_{1.05}$. The ratio between the intensities of the typical octahedral and tetrahedral aluminum chemical shifts was 1.4:1, which was completely different from the ratio observed for pure kaolinite (400:1). These results supported the hypothesis that Al(III) was partially removed from the gibbsite octahedral sheet, to induce formation of the aluminum(III) phthalocyanine. In other words, kaolinite served as support, catalyst, and source of Al(III) ions.

3.9. Textural analysis

Specific surface area calculated by BET (Table 2) shown that intercalation with DMSO and $PCNO_2$ grafting procedures to generate metallophthalocyanines induces a decreasing of the specific surface area, on other hand the pore size of the grafted compound Ka-$PCNO_2$ is bigger than for purified kaolinite (179 Å) with a value of 730 Å. In this sense the presence of large organic molecules such as Al(III)TNPMPc promotes the exposure of the interlayer hydroxyl groups inducings in all cases the decrease of specific surface area and increase of pore size, probably because the pores that were originated by intercalated DMSO molecules (anchored only by hydrogen bonds) into kaolinite structures were completely removed before $PCNO_2$ grafting. The changes in surface area values may be related to the stacking/restacking of kaolinite and Al(III) TNPMc complexes immobilization in situ and also to delamination of Ka-PCNO platelets that induces the textural changes of kaolinite.

4. Conclusion

FTIR, XPS and UV/Vis spectroscopy confirmed the one-step synthesis and immobilization of a metallophthalocyanine on kaolinite, with the clay serving as support/catalyst. XRD and SEM analyses showed that the kaolinite structure became disorganized during the synthesis. This disorganization was later confirmed by NMR—octahedral Al(III) ions dissolved in the reaction medium and promoted metallophthalocyanine cyclomerization in the presence of pthalonitrile. This process constitutes a new route for metallophthalocyanine synthesis that meets the principles of green chemistry and sustainability.

Acknowledgements

The authors thank the Brazilian funding agencies FAPESP (2013/19523-3), CAPES, and CNPq and Prof. Tiago Venâncio (Universidade Federal de São carlos) for assistance with ^{27}Al nuclear magnetic resonance analyses.

References

[1] Kaya EÇ, Karadeniz H, Kantekin H. The synthesis and characterization of metal-free and metallophthalocyanine polymers by microwave irradiation containing diazadithiamacrocyclic moieties. Dyes Pigments 2010;85:177–82.

[2] Zawadzka A, Plóciennik P, Strzelecki J, Korcala A, Arof AK, Sahraoui B. Impact of annealing process on stacking orientations and second order nonlinear optical properties of metallophthalocyanine thin films and nanostructures. Dyes Pigments 2014;101:212–20.

[3] Karl MK, Kevin MS, Roger G. Spectroscopic and electrochemical characterization the porphyrin handbook: phthalocyanines, vol XXVI. London: Academic Press; 2002.

[4] Mutsumi K, Takahisa K, Kazuchika O, Kenji H, Hirofusa S, Nagao K. Self-organization of hydrogen-bonded optically active phthalocyanine dimers. Langmuir 2003;19:4825–30.

[5] Gürek AG, Hirel C. Photosensitizers in medicine, environment and security. 2012.

[6] Mack J, Kobayashi N. Low symmetry phthalocyanines and their analogues. Chem Rev 2011;111:281–321.

[7] Lukyanets EA, Nemykin VN. The key role of peripheral substituents in the chemistry of phthalocyanines and their analogs. J Porphyr Phthalocya 2010;14:1–40.

[8] Oliveira E, Neri CR, Ribeiro AO, Serra OA, Yamamoto Y, Garcia VS, Costa LL, Prado AGS, Moua AO. Hexagonal mesoporous silica modified with copper phthalocyanine as a photocatalyst for pesticide 2,4-dichlorophenoxiacetic acid degradation. J Colloid Interf Sci 2008;323:98–104.

[9] Ernst S, Selle M. Immobilization and catalytic properties of perfluorinated ruthenium phthalocyanine complexes in MCM-41-type molecular sieves. Micropor Mesopor Mat 1999;27:355–63.

[10] da Silva TH, de Souza TFM, Ribeiro AO, Ciuffi KJ, Nassar EJ, Silva MLA, et al. Immobilization of metallophthalocyanines on hybrid materials and in-situ synthesis of pseudo-tubular structures from an aminofunctionalized kaolinite. Dyes Pigments 2014;100:17–23.

[11] Bhattacharyya KG, Gupta SS. Adsorption of a few heavy metals on natural and modified kaolinite and montmorillonite: a review. Adv Colloid Interfac 2008;140:114–31.

[12] Avila LR, de Faria EH, Ciuffi KJ, Nassar EJ, Calefi PS, Vicente MA, et al. New synthesis strategies for effective functionalization of kaolinite and saponite with silylating agents. Colloid Interf Sci 2010;341:186–93.

[13] Yang S, Yuan P, He H, Qin Z, Zhou Q, Zhu J, et al. Effect of reaction temperature on grafting of γ-aminopropyltriethoxysilane (APTES) onto kaolinite. Appl Clay Sci 2012;62–63:8–14.

[14] Machado GS, Groszewicz PB, Castro KADF, Wypych F, Nakagaki S. Catalysts for heterogeneous oxidation reaction based on metalloporphyrins immobilized on kaolinite modified with triethanolamine. J Colloid Interf Sci 2012;374:278–86.

[15] Bizaia N, de Faria EH, Ricci GP, Calefi PS, Nassar EJ, et al. Porphyrin-kaolinite as efficient catalyst for oxidation reactions. ACS Appl Mater Interfaces 2009;11:2667–78.

[16] De Faria EH, Nassar EJ, Ciuffi KJ, Vicente MA, Trujillano R, Rives V, Calefi PS. New highly luminescent hybrid materials: terbium pyridine-picolinate covalently grafted on kaolinite. ACS Appl Mater Interfaces 2011;3:1311–8.

[17] de Faria EH, Ciuffi KJ, Nassar EJ, Vicente MA, Trujillano R, Calefi PS. Novel reactive amino-compound: tris(hydroxymethyl)aminomethane covalently grafted on kaolinite. Appl Clay Sci 2010;48:516–21.

[18] Shaposhnikov GP, Maizlish VE, Kulinich VP. Synthesis and properties of extracomplexes of tetrasubstitued phthalocyanines. Russ J Gen Chem 2005;75:1830–9.

[19] Karaoglan GK, Gumrukçu G, Koca A, Gul A, Avcıata U. Synthesis and characterization of novel soluble phthalocyanines with fused conjugated unsaturated groups. Dyes Pigments 2011;90:11–20.

[20] Bahadoran F, Dialameh S. Microwave assisted synthesis of substituted metallophthalocyanines and their catalytic activity in epoxidation reaction. J Porphyr Phthalocya 2005;9:163–9.

[21] Zhou X, Li J, Wang X, Jin K, Ma W. Oxidative desulfurization of dibenzothiophene based on molecular oxygen and iron phthalocyanine. Fuel Process Technol 2009;90:317–23.

[22] NIST X-ray Photoelctron SpectroscopCy Database, AV. Naumkin, A. Kraut-Vass, S.W. Gaarenstroom, C.J. Powell, NIST standard reference Database 20, v. 4.1: htttp://srdata.nist.gov/XPS/.

[23] Valášková M, Rieder M, Matějka V, Čapková P, Slíva A. Exfoliation/delamination of kaolinite by low-temperature washing of kaolinite–urea intercalates. Appl Clay Sci 2007;35:108–18.

[24] Nakagaki S, Machado GS, Halma M, Marangon AAS, Castro KADF, Mattoso N, et al. Immobilization of iron porphyrins in tubular kaolinite obtained by an intercalation/delamination procedure. J Catal 2006;242:110–7.

[25] Araújo FR, Baptista JG, Marçal L, Ciuffi KJ, Nassar EJ, Calefi PS, et al. Versatile heterogeneous dipicolinate complexes grafted into kaolinite: catalytic oxidation of hydrocarbons and degradation of dyes. Catal Today 2014;227:105–15.

[26] Silva TH, Reis MJ, Faria EH, Ciuffi KJ, Nassar EJ, Calefi PS. Study of reliability of thermal analysis technique in the quantification of organic material in physical mixture of kaolinite and tris(hydroxymethyl)aminomethane. Braz J Therm Anal 2012;01:15–22.

[27] de Faria EH, Lima OJ, Ciuffi KJ, Nassar EJ, Vicente MA, Trujillano R, et al. Hybrid materials prepared by interlayer functionalization of kaolinite with pyridine-carboxylic acids. J Colloid Interf Sci 2009;335:210–5.

[28] Letaief S, Elbokl TA, Detellier C. Reactivity of ionic liquids with kaolinite: melt intersalation of ethyl pyridinium chloride in an urea-kaolinite pre-intercalate. J Colloid Interf Sci 2006;302:254–8.

[29] Fitzgerald JJ, Hamza AI. Solid-state 27Al and 29Si NMR studies of the reactivity of the aluminum-containing clay mineral kaolinite. Solid State Ionics 1989;32/33:378–88.

[30] Mantovani M, Escudero A, Becerro AI. Influence of OH− concentration on the illitization of kaolinite at high pressure. Appl Clay Sci 2011;51:220–5.

[31] Lyubimtsev AV, Zheglova NV, Smirnova EN, Syrbu SA. Reactivity of phthalocyanine precursors. Russ Chem Bull Int Ed 2015;64:1933–41.